# ANALYSIS OF SPATIAL SCHEDULING IN DOWNLINK VEHICULAR COMMUNICATIONS: SUB-6 GHZ VS MMWAVE

Mehdi Haghshenas[1], Francesco Linsalata[1], Luca Barbieri[1], Mattia Brambilla[1], Monica Nicoli[2], Maurizio Magarini[1]
[1]Dipartimento di Elettronica, Informazione e Bioingegneria, Politecnico di Milano, Via Ponzio 34/5, 20133, Milano, Italy,
[2]Dipartimento di Ingegneria Gestionale, Politecnico di Milano, Via Lambruschini, 4/B, 20156, Milano, Italy

NOTE: Corresponding author: Mehdi Haghshenas, mehdi.haghshenas@polimi.it

***Abstract*** – *Vehicular communications are gaining a lot of attention for the delivery of enhanced mobility services that require multi-Gbps and low latency connections. In this paper, we focus on Infrastructure-to-Vehicle (I2V) communications where a gNB has to assign spatial resources to a number of connected vehicle users. To efficiently manage the scheduling, we compare the Zero Forcing (ZF) and Maximum Ratio (MR) precoding strategies by evaluating the effect of shifting from sub-6 GHz to millimeter wave (mmWave) frequencies in urban and highway mobility scenarios. We analyze the impact of the geometry of the environment and propagation characteristics at different frequencies in terms of number of users that can be served and spectral efficiency. To model the I2V channel, we integrate realistic traffic conditions generated by SUMO into an accurate channel model based on ray tracing software by WirelessInsite. By numerical results we demonstrate the degradation at mmWave compared to sub-6 GHz on the multiplexing gain. We show the higher efficiency of ZF compared to MR as the former is not limited by inter-user interference, especially in urban scenarios where the number of distinctive eigendirections in space is limited. On the other hand, highway mobility has a more uniform distribution of vehicles that can be conveniently explored by the ZF scheduling to serve more users. Lastly, we show the benefits of adopting a higher number of transmit antennas at mmWave jointly with efficient scheduling to achieve higher spectral efficiency.*

**Keywords** – 5G, channel orthogonality, I2V, maximum ratio, mmWave, spatial resource scheduling, zero forcing

## 1. INTRODUCTION

The integration of dedicated communication technologies within current automotive ecosystems is expected to enable faster, safer, and greener mobility [1, 2]. Among the recent technological advances, Vehicle-to-Everything (V2X) networking paradigms [3, 4, 5] are foreseen as disruptive, being designed to transfer multi-Gbps data streams and ultra-reliable and low-latency communications [6, 7, 8]. Rooted in 5G [9, 10] and following the related evolution towards 6G [11, 12, 13], they are conceived to support direct interactions among vehicles and road infrastructures via Vehicle-to-Vehicle (V2V) and Vehicle-to-Infrastructure (V2I) communications [14, 15], while enabling a wide range of vehicular use cases [16, 17, 18, 19]. Among them, it is worth mentioning cooperative perception and planning strategies, platooning, and advanced driving [20]. Despite the far-reaching possibilities introduced by V2X networking, sophisticated processing tools, efficient resource allocation strategies, as well as novel frequency bands are needed to meet the stringent requirements imposed by safety-critical autonomous driving applications [21].
Nowadays, the research interest is focusing on millimeter wave (mmWave) frequencies [22, 23] for accommodating the ever-increasing demand of communication resources for V2X use cases, providing a remedy to the oversaturated bands at sub-6 GHz [24]. The wide spectrum availability makes them ideal to support fast, reliable, and ultra-wide bandwidth connections between vehicles, infrastructures and road users. Nevertheless, when compared to standardized cellular sub-6 GHz systems, they face more propagation challenges as the mmWave signal is subject to higher propagation and penetration losses. Massive Multiple-Input-Multiple-Output (MIMO) antenna systems are deployed to counteract such detrimental effects by using collimated spatial beams and concentrate the transmission power towards the receiver [25, 26, 27, 28, 29].

At mmWaves, the conventional spatial multiplexing strategies developed for sub-6 GHz cellular technologies may not be equally performing as the channel propagation characteristics significantly differ. Indeed, mmWave channels tend to be constituted by a few dominant clustered paths with sparse algebraic structure [30, 31]. Moreover, the large number of antenna elements employed at these frequencies limit the classic processing methodologies for sub-6 GHz, e.g., precoding, and demand new design strategies [32]. These effects are further exacerbated when considering highly dynamic environments, and in particular vehicular networks, where these operations should be implemented on a very short periodic basis [33]. The next generation of mobile cellular stations, i.e., gNBs, should implement intelligent spatial scheduling techniques to guarantee a fair access to the available communication resources for all connected users.

### Paper contribution

In this paper, we explore the problem of spatial scheduling at mmWaves and compare it with respect to the sub-6 GHz case, thus examining the effect of a completely different propagation condition (the mmWave channel is by far more sparse than the sub-6 GHz one). In our previous work [34], we demonstrated that the spatial resources, or equivalently, spatial multiplexing efficiency in the mmWave band is lower compared to the common uncorrelated Rayleigh channel model. However, there are still some aspects left behind to be examined further. Therefore, in this paper we aim to expand our previous investigation by adding the following contribution:

- a deeper analysis of the multiplexing gain loss at mmWave with respect to sub-6 GHz band;
- the design and implementation of a more realistic channel model based on WirelessInsite [35] in place of a generic Rayleigh channel model; it allows us to realistically evaluate the position-dependent channel for both mmWave and sub-6 GHz frequencies;
- the analysis on the eigen-structure of the channel correlation matrix to witness the differences between mmWave and sub-6 GHz propagation and its impact over the multiplexing gain;
- the analysis in two practical Infrastructure-to-Vehicle (I2V) scenarios, namely highway and urban environments, to demonstrate the impact of the environment geometry on the multiplexing gain;
- the analysis on the impact of antenna configuration (such as $8 \times 8$ and $32 \times 32$ Uniform Planar Arrays (UPAs)) and associated beam resolution on spatial multiplexing;
- the comparison of two precoders, i.e., Zero Forcing (ZF) and Maximum Ratio (MR), over all simulations to quantify the effect of interference on spatial multiplexing at the mmWave band.

The I2V context is examined for urban and highway mobility conditions, which are characterized by time-varying traffic densities and different vehicles' speeds. Realistic traffic patterns are obtained using a traffic simulator and are used as input to an electromagnetic ray-tracer to obtain the corresponding channel impulse response at both mmWave and sub-6 GHz frequencies. The analysis targets to quantify the degradation of two widely used linear precoders, namely ZF and MR, in case of moving from the sub-6 GHz frequency region (for which they have been demonstrated to be extremely efficient) to mmWave. By numerical simulations we show that mmWaves incur a lower spatial multiplexing gain due to the sparsity of the channel (and confirmed by a faster decay of the magnitude of eigenvalues); ZF outperforms MR thanks to its interference-suppression capability; and that MIMO systems with a large number of antenna elements are needed to significantly increase the spectral efficiency and let the gNB serve a higher number of users.

### Paper structure

The structure of the paper is as follows. Section 2 presents an overview of spatial scheduling algorithms while Section 3 details the system model and linear precoders considered in this paper. Section 4 discusses the semi-orthogonal user selection algorithm. Section 5 explains the simulation framework while the numerical results are in Section 6. Lastly, Section 7 concludes the paper.

### Paper notation

Uppercase boldface letters stands for matrices and lowercase boldface for vectors. Symbol $||\cdot||$ represents the Euclidean norm operator, $|\cdot|$ is the absolute value or the cardinality of a set according to the input variable, $(\cdot)^*$ stands for the conjugate transpose, and $(x)^+ = \max(x, 0)$. $\mathbf{H}^\dagger$ is the pseudo-inverse of $\mathbf{H}$. Operation $\mathbb{E}\{\cdot\}$ indicates the expected value. Lastly, $\mathcal{N}_{\mathbb{C}}(\mu, \sigma^2)$ denotes a circularly-symmetric complex Gaussian distribution with mean and variance equal to $\mu$ and $\sigma^2$, respectively.

## 2. RELATED WORK

Spatial scheduling in V2X systems has been addressed in several papers in the literature, where a variety of algorithms have been proposed. Complete surveys on resource allocation in vehicular networks are in [14, 15, 36], where most of the existing algorithms are compared in V2X scenarios.

The Proportional Fair (PF) scheme with its related adaptations is probably a largely adopted solution in wireless networks [37, 38]. It is optimal for stationary channels and, in addition, it is able to consider and exploit the users' channel diversity. However, V2X communications are characterized by non-stationary channels [39, 40, 41], and the temporal duration of a connection with a gNB can be very short (few seconds) [42]. For this reasons, PF easily loses its efficacy. To enhance the PF scheduler performance, authors in [43] introduced a data rate prediction mechanism that exploits mobility information. A real dataset was used to quantify the performance gain which amounts to an increased throughput of 15%-55% with respect to the traditional PF scheduler.

With the increasing number of antennas, it is easier to experience independent channels across multiple users served by a gNB, and the classical linear precoding schemes (e.g., ZF) can obtain a good performance, still keeping the complexity low. The algorithm for user group selection with ZF is detailed in [44], [45], and [46]. However, those works [44, 45, 46] assumed Rayleigh fading channels, an assumption that fails in case of mmWave channels. In [47] and [48], the authors proposed an algorithm for user subset selection by ZF, but they did not enforce semi-orthogonality across users as they address the problem of cancelling the interference by dirty

paper coding. In [49], a low complexity scheduling algorithm with block diagonalization was proposed to eliminate inter-user interference with perfect channel state in- formation since the transmitter decomposes a multiuser MIMO channel into multiple parallel independent single- user MIMO channels. For a large number of users, the transmitter only selects the best quality served users to maximize the system throughput. The authors of [50] proposed an efficient scheduling algorithm for downlink MIMO systems using ZF beamforming to achieve high system throughput with low computational complexity. Based on a theoretical approach, they represented the system as a graph and formulate the scheduling problem as a maximum weight k-colorable subgraph problem. Additionally, [51] employed different precoders along with max-min power control to investigate achieved spectral efficiency in the context of cell-free massive MIMO with centralized and distributed precoder design. Most of the above-mentioned works lack in terms of realistic simulation methodology, application to a real use case, e.g., vehicular network and, most notably, they do not deal with mmWave signal propagation. By contrast, in this paper, we analyze the benefits and limits of two different spatial scheduling algorithms, i.e., ZF and MR, by exploiting an accurate position-based ray tracer for channel model in two vehicular environments (urban and highway) at both sub-6 GHz and mmWaves, showing how the latter strongly impact the multiplexing efficiency.

## 3. SYSTEM MODEL

In this section, we first detail the model for a multi-antenna communication system in Section 3.1, then in Section 3.2 we define the spectral efficiency objective function to be optimized by ZF and MR precoders.

### 3.1 Communication system

We consider a single cell scenario with $K$ single antenna receivers (i.e., vehicle users) served by a gNB. The gNB is responsible for allocating all the radio resources. The gNB is equipped with a UPA of $I$ antennas overall, which allows the transmission of up to $I$ independent streams via spatial multiplexing. The array is arranged along the $yz$- plane, with $A$ and $B$ elements on $y$ and $z$ axes such that $A \times B = I$. The transmit array response vector $\mathbf{a}_T(\vartheta_n, \phi_n) \in \mathbb{C}^{I\times 1}$ for a single path $n$ is thus [52]

$$\mathbf{a}_T(\vartheta_n,\phi_n) = \frac{1}{\sqrt{I}}\left[1,\cdots,\mathrm{e}^{j\ell d(a\sin\vartheta_n\sin\phi_n + b\cos\phi_n)},\cdots \right.$$
$$\left.\cdots,\mathrm{e}^{j\ell d((A-1)\sin\vartheta_n\sin\phi_n+(B-1)\cos\phi_n)}\right]^{\mathrm{T}}, \quad (1)$$

where the indexes $a$ and $b$ identify a single antenna element along $y$ and $z$ axes, respectively, $\ell = 2\pi/\lambda$, $\lambda$ is the wavelength, $d$ is the inter-element spacing, and $(\vartheta_n, \phi_n)$ is the pair of Angles of Departure (AODs), in terms of azimuth and elevation, from the gNB.

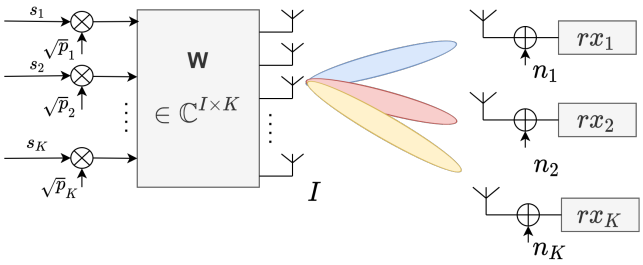


**Fig. 1** – Block diagram of the multiuser multiple input single output channel.

The downlink channel vector $\mathbf{h}_k \in \mathbb{C}^{1\times I}$ for each user $k$ is defined as

$$\mathbf{h}_k = \sum_{n=1}^{N_{p,k}} \alpha_n \mathbf{a}_T^*(\vartheta_n,\phi_n), \quad k = 1\cdots K, \quad (2)$$

where, $\alpha_n$ denotes the channel complex coefficient for the $n$-th path, while $N_{p,k}$ is the total number of paths between gNB and user $k$. By collecting the downlink channels of all $K$ users into one matrix $\mathbf{H} = [\mathbf{h}_1^{\mathrm{T}},\cdots,\mathbf{h}_K^{\mathrm{T}}]^{\mathrm{T}} \in \mathbb{C}^{K\times I}$, we can write the linear transformation model for the multiuser system as

$$\mathbf{y} = \mathbf{H}\mathbf{x} + \mathbf{n} = \mathbf{H}\mathbf{W}\mathbf{P}\mathbf{s} + \mathbf{n}, \quad (3)$$

where $\mathbf{y} \in \mathbb{C}^{K\times 1}$ is the collective received symbol for all users, $\mathbf{n} = [n_1,\cdots,n_K]^{\mathrm{T}} \in \mathbb{C}^{K\times 1}$ is the additive complex white Gaussian noise, with each element $n_k$ independently drawn from $\mathcal{N}_{\mathbb{C}}(0,\sigma_n^2)$, and $\mathbf{x} \in \mathbb{C}^{I\times 1}$ is the transmitted signal from gNB at a specific time instant. Let $\mathbf{s} = [s_1,\cdots,s_K]^{\mathrm{T}}$ with $s_k \sim \mathcal{N}_{\mathbb{C}}(0,1)$, $\mathbf{w}_k \in \mathbb{C}^{I\times 1}$, and $P_k$ be the collective transmitted symbol, beamforming precoder, and associated power to user $k$, respectively, with $\mathbf{W} = [\mathbf{w}_1,\cdots,\mathbf{w}_K]$ and $\mathbf{P} = \mathrm{diag}\left(\left[\sqrt{P_1},\cdots,\sqrt{P_K}\right]\right)$ being the collective matrix form of precoders and users' powers. Therefore, the transmitted signal from gNB is $\mathbf{x} = \sum_{k=1}^{K}\sqrt{P_k}\mathbf{w}_k s_k$ and, accordingly, the received symbol for user $k$ is:

$$y_k = (\sqrt{P_k}\mathbf{h}_k\mathbf{w}_k)s_k + \sum_{j\neq k}\sqrt{P_j}\mathbf{h}_j\mathbf{w}_j s_j + n_k, \quad (4)$$

where the first term on the right hand side is the desired signal for the intended user $k$, and the second term is the undesired interference. Accordingly, the equivalent block diagram of the described communication system is illustrated in Fig. 1.

### 3.2 Spectral efficiency and downlink precoders

In this section, we first briefly review two well-known precoders, i.e., ZF and MR, which we consider in our analysis as they provide low computational complexity. For

an I2V communication system with $I$ antennas at gNB and $K$ users to be served, the computational complexity for ZF and MR is $O(K^2 I)$ and $O(K)$, respectively [53].
In the literature, ZF is acknowledged as the suboptimal solution to determine a beamforming precoder that satisfies the zero-interference condition across users, i.e., $\mathbf{h}_k^{\mathrm{T}}\mathbf{w}_j = 0$ for $j \neq k$. A choice of $\mathbf{W}$ that fulfills the zero-interference condition across the set of selected users $S \subseteq K$ by gNB scheduler is given by:

$$\mathbf{W}(S) = \frac{\mathbf{H}(S)^{\dagger}}{\|\mathbf{H}(S)^{\dagger}\|} = \frac{\mathbf{H}(S)^{*}(\mathbf{H}(S)\mathbf{H}(S)^{*})^{-1}}{\|\mathbf{H}(S)^{*}(\mathbf{H}(S)\mathbf{H}(S)^{*})^{-1}\|}, \quad (5)$$

where $\mathbf{H}(S)$ is the corresponding sub-matrix of $\mathbf{H}$. The normalization is applied to achieve $\mathbb{E}\{\|\mathbf{w}_k\|^2\} = 1$. Additionally, MR is the simplest precoder in MIMO systems where no matrix inversion is required. The MR intrinsically tries to maximize the gain for the respective user without any interference suppression over the others. The precoder matrix for MR is evaluated as:

$$\mathbf{W}(S) = \frac{\mathbf{H}^{*}(S)}{\|\mathbf{H}(S)\|}, \quad (6)$$

where the normalization is done again to achieve $\mathbb{E}\{\|\mathbf{w}_k\|^2\} = 1$. The normalization is essential to provide a fair comparison among two precoders which will be discussed in Section 6. Following the input-output model in *(4)*, the achievable downlink Spectral Efficiency (SE) for each user $k$ is computed by considering the interference as noise [53] as follows:

$$SE_k = \log_2\left(1 + \frac{P_k|\mathbf{h}_k\mathbf{w}_k|^2}{\sum_{\substack{s\in S\\ s\neq k}} P_s|\mathbf{h}_k\mathbf{w}_s|^2 + n_k}\right), \quad (7)$$

and the total achievable downlink spectral efficiency is:

$$R(S) = \max_{P_s:\sum_{i\in S} P_s \leq P} \sum_{s\in S} SE_s, \quad (8)$$

where $P_s$ is the transmitted power being assigned to the selected user $s \in S$ and $P$ is the available power to be assigned by the gNB. The optimal power allocation $P_s$ can be achieved by water-filling, where the power $P$ is distributed among the users according to their channel quality, i.e., allocating lower power to the users with higher noise. The associated power is evaluated as [54]:

$$P_s = \left(\mu - \frac{\sigma_n^2}{\|\mathbf{h}_s\|^2}\right)^{+}, \quad (9)$$

where the water level $\mu$ is calculated by solving

$$\sum_{s\in S}\left(\mu - \frac{\sigma_n^2}{\|\mathbf{h}_s\|^2}\right)^{+} = P. \quad (10)$$

It should be noted that for the deterministic channel $\mathbf{H}$, the optimum value for *(8)* can be achieved by applying water-filling over the eigenvalues of $\mathbf{H}\mathbf{H}^{*}$ with power constraint of $P$ [54]. However, finding the optimal subset of users that maximized the achievable rate is computationally expensive and requires a brute force search. Therefore, in the next section, we explain the developed algorithm for the selection of users $S \subseteq K$, by considering a constraint on the orthogonality across them.

## 4. SEMI-ORTHOGONAL USER SELECTION

In this section, we explain how a subset $S \subseteq K$ of users is selected. Only after this step, the precoder matrices *(5)* and *(6)* can be built and it is possible to use water-filling to maximize the system capacity in *(8)*. The following algorithm guarantees a specific level of orthogonality among users, which determines the level of interference a user causes to another one. As will be stressed later on in Section 6 for the MR precoder, orthogonal channels are beneficial to lower the mutual interference. Let us denote with $S$ the dynamic set of selected users that has to be served by the gNB. The user selection from the gNB is based on an iterative algorithm. The single iteration is denoted with $i$, while $T_i$ is the set of non-selected users at iteration $i = 1, \ldots, I$. Initially, $T_1 = K$ (i.e., it contains all $K$ users), while $S$ is empty. At iteration $i$, for each user $k \in T_i$, the algorithm computes $\mathbf{g}_k$, the orthogonal component of $\mathbf{h}_k$ to the subspace spanned by already selected users $\{\mathbf{g}_{(1)}, \cdots, \mathbf{g}_{(i-1)}\}$ as:

$$\mathbf{g}_k = \mathbf{h}_k\left(\mathbf{I} - \sum_{j=1}^{i-1}\frac{\mathbf{g}_{(j)}^{*}\mathbf{g}_{(j)}}{||\mathbf{g}_{(j)}||^2}\right), \quad (11)$$

where $\mathbf{g}_{(j)}$ corresponds to the orthogonal channel component of the user selected at iteration $j$, and for the first iteration we set $\mathbf{g}_k = \mathbf{h}_k$. Afterwards, the algorithm chooses the user with the strongest orthogonal channel component as:

$$\pi(i) = \arg\max_{k\in T_i} \|\mathbf{g}_k\|. \quad (12)$$

Next, the algorithm checks if adding the current new candidate in the system can increase the system capacity in *(8)*. If the capacity is increased, then the candidate is added to $S$, and $\mathbf{g}_{(i)} = \mathbf{g}_{\pi(i)}$. If $|S| < I$ a new set for the next iteration is evaluated by considering the following orthogonality constraint

$$T_{i+1} = \left\{k \in T_i, k \neq \pi(i) | \frac{|\mathbf{h}_k\mathbf{g}_{(i)}^{*}|}{\|\mathbf{h}_k\| \cdot \left\|\mathbf{g}_{(i)}\right\|} \leq \beta\right\}, \quad (13)$$

where $\beta$ is the semi-orthogonality threshold, which assumes a value between 0 and 1 (0 means perfect orthogonality). If the constraint is satisfied for a user, then it

**Algorithm 1** User selection algorithm.

Initialize $T_1 = \{1, ..., K\}$, $S = \emptyset$, $i = 1$.
**while** $|S| \leq I$ and $T_i \neq \emptyset$ **do**
  **if** $i = 1$ **then**
    $\mathbf{g}_k = \mathbf{h}_k, \forall k \in T_1$
  **else**
    Compute $\mathbf{g}_k$ according to *(11)*, $\forall k \in T_i$
  **end if**
  Select the best user according to

$$\pi(i) = \arg\max_{k \in T_i} ||\mathbf{g}_k||$$

  Calculate $\Delta R = R(S \cup \pi(i)) - R(S)$ following *(8)*.
  **if** $\Delta R > 0$ **then**
    $S \leftarrow S \cup \{\pi(i)\}$
    $\mathbf{g}_{(i)} = \mathbf{g}_{\pi(i)}$
    Update $T_{i+1}$ according to *(13)*
    $i \leftarrow i + 1$
  **else**
    Break.
  **end if**
**end while**

is added to $T_{i+1}$ for the next iteration; otherwise, it is discarded. The complete algorithm for user selection is summarized in Alg. 1. Additionally, for $I > K$ the selection algorithm has a complexity of $O(2K^2)$ while for $I < K$ it is of $O(2KI)$.

## 5. SIMULATION METHODOLOGY

Spatial scheduling schemes are here evaluated using a simulation framework that supports the flexible configuration of environments, vehicle types and densities, as well as electromagnetic propagation properties. Inspired by the simulator in [55], we integrate realistic traffic, real-world maps and an electromagnetic solver to reliably characterize radio frequency propagation for I2V communications. Specifically, we integrate SUMO [56] and OpenStreetMap [57] to model vehicular traffic over real road networks, and WirelessInsite [35] to obtain the position-dependent channel impulse response along with channel coefficients and AoDs as in *(2)*. By taking as input the positions, velocities and headings of all vehicles from SUMO and the coordinates of the gNB, WirelessInsite enables a realistic modeling of the I2V channel at both mmWave and sub-6 GHz frequencies, which are then used to evaluate the performance of the spatial multiplexing strategies described in Section 4.

To analyze the effect of traffic patterns and the impact of vehicular mobility, we consider two different I2V scenarios, namely:

1. an urban environment in the city of Rosslyn, Virgina, USA;

2. a type C highway (dual carriageway) in Milan, Italy.

Figures 2a and 2b report a screenshot of the WirelessInsite simulator in both urban and highway scenarios, respectively, where the gray blocks represent buildings while vehicles are in red. Three roads characterize the urban settings, while a single $400$ m long road is considered for the highway. Both scenarios support two-way lanes that allow vehicles to enter/exit the simulation from top/bottom, for the urban environment, and left/right for the highway. In this regard, Fig. 3 exemplifies four possible trajectories in the urban area. To consider the same number of vehicle users to be served by the gNB, we set to $30$ the number of connected vehicles that are present in the scenario. In case the traffic demand results in a higher number of vehicles, the exceeding vehicles are considered as potential blockers. Due to the randomness of trajectories, any vehicle that exits the scenario is randomly replaced by another one. The gNB (green cube) is located in the center of each environment.

The main parameters characterizing vehicles' mobility, simulation duration, and geometric properties of the environments are summarized in Table 1. Identical trajectories and gNB positions are considered for a fair comparison between mmWave and sub-$6$ GHz.

**Table 1** – Simulation parameters for urban and highway scenarios.

| Parameter | Urban | Highway |
|---|---|---|
| Sampling time | 1 s | 1 s |
| Duration of simulation | 100 s | 100 s |
| Traffic flow | 1.5 veh/s | 3.5 veh/s |
| Maximum speed | 50 km/h | 80 km/h |
| Area | 500x200 m | 600x500 m |

Regarding the parameters for channel simulation in WirelessInsite, we select a frequency of $3.6$ GHz for sub-$6$ GHz channels, and $28$ GHz for mmWave. The signal bandwidth is $20$ MHz, while the noise power is $\sigma_n^2 = -81$ dBm. All vehicles are assumed to have an isotropic antenna placed at $15$ cm above the vehicle roof, while the gNB is equipped with an $8 \times 8$ UPA (unless otherwise specified). Moreover, the channel is assumed to be perfectly known at the gNB and the total average power at the transmitter is $P = 20$ dBW.

## 6. NUMERICAL RESULTS

In this section, we present and analyze numerical results to demonstrate how mmWave propagation characteristics affect scheduling in the spatial domain with respect to conventional sub-$6$ GHz channels. Moreover, we aim to analyze the impact of orthogonality constraint $\beta$ in *(13)* on ZF and MR precoders.

Fig. 4 shows the averaged number of selected users for the ZF (dotted line) and MR (dashed line) precoders, in both urban (red color) and highway (blue color) scenarios and for both sub-$6$ GHz and mmWave frequencies, with respect to orthogonality threshold $\beta$. We recall that $\beta$ defines the orthogonality constraint among users *(13)*, and that $\beta = 0$ means perfect orthogonality. Increasing the value of $\beta$ (from $0$ to $1$) implies accepting interference

**(a)** Urban scenario, Rosslyn, Virginia, USA.

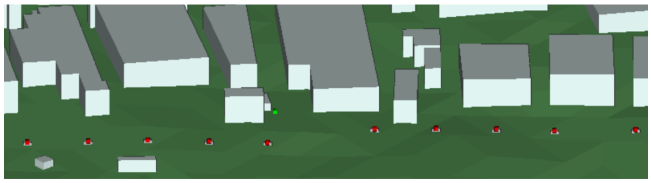

**(b)** Highway scenario, Milan, Italy.

**Fig. 2** – Simulated (a) urban and (b) highway scenario in WirelessInsite. Gray objects represent buildings while vehicles are in red. The green point is the gNB.

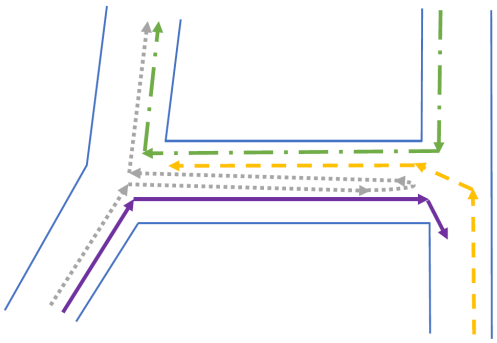

**Fig. 3** – Example of four possible trajectories in the urban scenario.

among the users' channel while establishing a candidate list for the next iteration of user selection. The analysis suggests that a relaxation of the orthogonality constraint has a different impact on the two precoders. Indeed, for the MR precoder, the number of selected users initially increases but then it saturates. On the other hand, for ZF, we experience a monotonic increase of selected users. The different behavior and impact of $\beta$ can be explained by investigating the intrinsic characteristics of each precoder. Potentially, ZF is able to suppress the interference while increasing the spectral efficiency for all users; while MR seeks to maximize the spectral efficiency for each user regardless of the interference level. Therefore, when above the specific orthogonality threshold constraint, the interference significantly affects the user selection algorithm, and it can strongly degrade the system performance and limit the number of users that a gNB can serve. In the same figure it is also possible to infer that the harsh propagation conditions of urban areas reduce the multiplexing gain. This behavior can be justified by visualizing the eigenvalues of the channel correlation matrix $\mathbf{H}\mathbf{H}^*$.

The magnitude of ordered eigenvalues is reported in Fig. 5 for both highway and urban scenarios over sub-

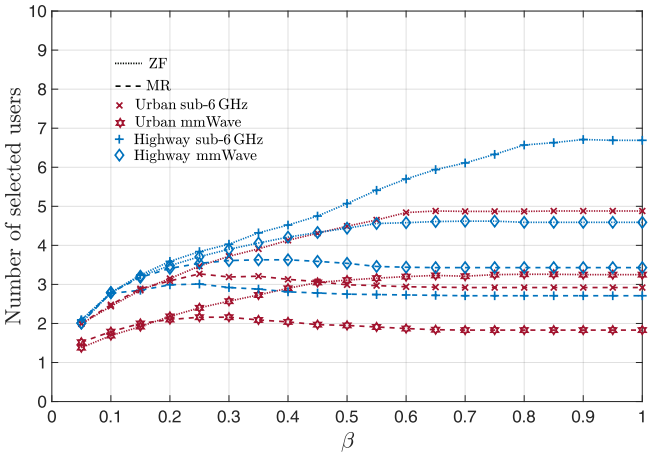


**Fig. 4** – Number of selected users using ZF and MR precoders in highway and urban environment over sub-6 GHz and mmWave band, and considering an $8 \times 8$ UPA at gNB.

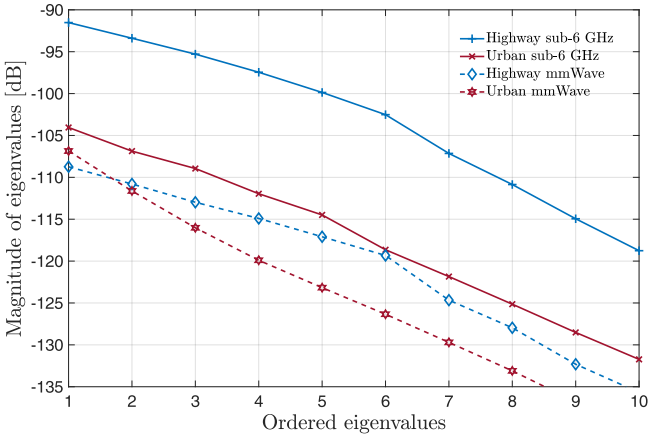


**Fig. 5** – Averaged eigenvalues for highway and urban scenario using a $8 \times 8$ UPA at gNB.

6 GHz and mmWave band. The values are obtained by aver- aging over all time instants. The faster decay of the curve for the urban scenario confirms that it is harder to have a high multiplexing gain, as opposed to a smoother trend for the highway case. As an example, the difference be- tween the first and fifth eigenvalues in the highway scenario for sub-6 GHz and mmWave is 8.34 dB and 8.35 dB, respectively, while in the urban scenario it is 10.44 dB and 16.31 dB, respectively. Moreover, for each scenario, the curve decays faster for mmWaves with respect to sub-6 GHz as they are more affected by blockage and penetration losses, and have less scatter points, i.e., the mmWave channel is more sparse. As a result, there are limited distinctive angles that the gNB can exploit to transmit to- ward vehicles. To further clarify this point, we employ the eigendecomposition of the channel correlation ma- trix as $\mathbf{H}\mathbf{H}^* = \mathbf{U}\Lambda\mathbf{U}^*$, where $\Lambda$ is the diagonal matrix of ordered eigenvalues, and $\mathbf{U}$ collects the associated eigen- vectors (or eigendirections). For each eigendirection, the corresponding eigenvalue determines the magnitude of the direction in space. A rapid decay of eigenvalues means that there are few significant directions in space

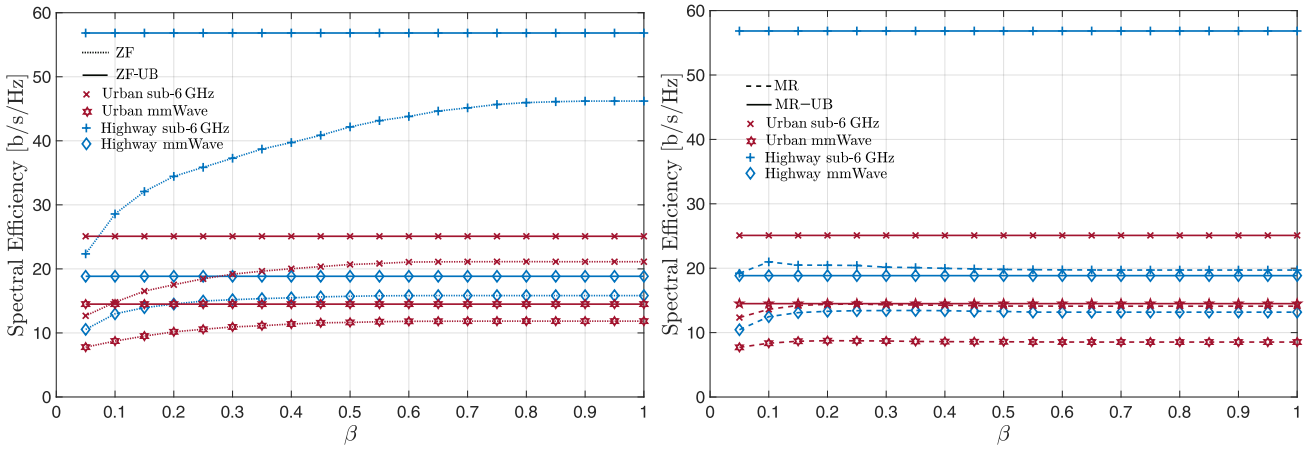


**(a)** ZF **(b)** MR

**Fig. 6** – Achievable spectral efficiency for (a) ZF and (b) MR precoders in highway and urban scenarios over sub-6 GHz and mmWave bands, and considering an $8 \times 8$ UPA at gNB. Solid lines represent the achievable Upper Bound (UB).

to be explored for spatial multiplexing, as only a limited number of good-quality channels can be used. All in all, it is possible to conclude that a lower number of users is served by the gNB at mmWave with respect to sub-6 GHz due to a lower number of resolvable spatial directions on the I2V link (from gNB to vehicles) that can be exploited for spatial multiplexing. To complement the analysis on the number of users that the gNB can serve, in Fig. 6 we report the achievable spectral efficiency *(8)* for sub-6 GHz and mmWave in urban and highway scenarios using the ZF (Fig. 6a) and MR (Fig. 6b) precoders. In both figures, we also represent the upper bound of spectral efficiency (solid lines) for all the simulated scenarios. Recalling Section 3, the upper bound is evaluated by applying water-filling over the eigenvalues of the channel correlation matrix $\mathbf{HH}^*$. Comparing Fig. 6a and Fig. 6b, we notice that ZF is able to get closer to the corresponding upper bound compared to MR. Moreover, comments in the previous paragraph on the impairments attributable to mmWave propagation are applicable in these figures as well. As a final analysis, we want to demonstrate the impact of antenna configuration on multiplexing gain at mmWave by considering two antenna array configurations at the gNB, i.e., $8 \times 8$ and $32 \times 32$ UPA. In fact, increasing the number of antennas facilitates the gNB capability of discriminating spatially-closed users that have similar AoD directions. Fig. 7 compares the two UPA configurations in terms of the number of selected users with respect to orthogonality constraint $\beta$ for mmWave I2V communications in urban and highway scenarios. By increasing the number of antennas it is possible to experience a higher multiplexing gain in both scenarios, with much higher gain for the ZF precoder rather than MR. With a $32 \times 32$ UPA, vehicles with adjacent AoDs can be distinguished at the gNB with a higher beam resolution. However, they are still prone to a high interference level. Therefore, a precoding mechanism with suppressing interference,

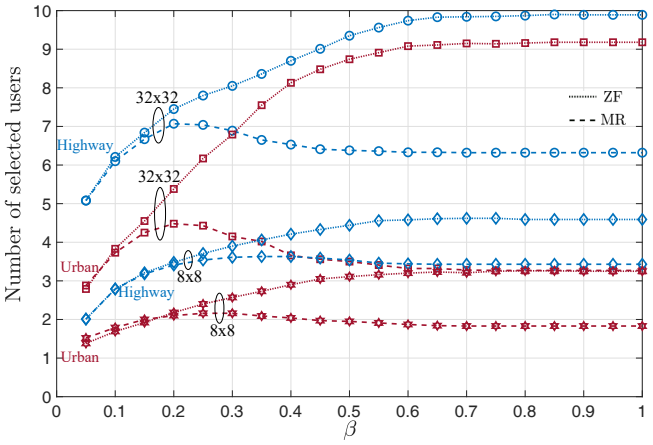


**Fig. 7** – Impact of antenna configuration ($8 \times 8$ vs $32 \times 32$ UPAs) on the number of selected users by a gNB at mmWave in highway and urban scenarios, for both ZF and MR precoders.

e.g. ZF, gets higher benefits from the increased number of antennas. Quantitatively, the ZF experiences an improvement of $\times$ 2.7 and $\times$ 2.1 on the number of selected users in urban and highway scenarios, respectively, while the values for MR are $\times$ 1.89 and $\times$ 1.91. In the case of ZF, the greater improvement in the urban scenario can be attributed to the urban building layout and geometry, where there are many vehicles with close AoDs that benefit more from a finer spatial beam resolution. Additionally, in Fig. 7, one may notice that an MR with $32 \times 32$ UPA saturates to the same number of users as the ZF with the $8 \times 8$ UPA configuration, confirming the higher efficiency of the ZF precoder.

Accordingly, Fig. 8 illustrates the corresponding spectral efficiency and the same effect can be observed here as well. To conclude the analysis on the results, a more sophisticated MIMO hardware allows us to have a higher beam resolution, enhanced user separability and higher multiplexing gain if, and only if, an appropriate precoder is employed. In other words, an inefficient choice on the

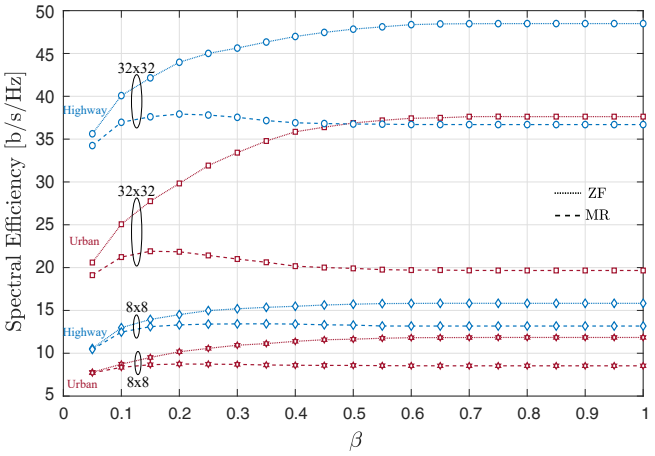


**Fig. 8** – Impact of antenna configuration ($8 \times 8$ vs $32 \times 32$ UPAs) on the achievable spectral efficiency by a gNB at mmWave in highway and urban scenarios, for both ZF and MR precoders.

precoding strategy can completely nullify the choice of a more complex hardware at gNB.

## 7. CONCLUSION

In this paper, we explored the performance of spatial scheduling by a gNB in I2V communications for urban and highway vehicular scenarios, and comparing mmWave and sub-$6$ GHz bands. We revealed that the geometry of the environment and propagation characteristics at different frequencies highly impact on the spatial multiplexing gain, which experiences a severe degradation when shifting from sub-$6$ GHz to mmWave frequencies. This outcome is justified by the spatial sparsity of the mmWave channel due to the propagation features in the environment. Indeed, in urban scenarios it is more difficult to separate users in space due to the closeness and overlapping of AoDs rather than for a highway. To overcome this issue, it is required to increase the number of antennas at the gNB, as it results in a higher beam resolution. However, the adoption of a simple precoder such as the MR has been demonstrated to be limited by the level of interference, and using an appropriate precoder such as the ZF is a more efficient choice. The ZF has been proved to outperform MR in both urban and highway scenarios, for both mmWave and sub-$6$ GHz, with remarkable improvements especially when a $32 \times 32$ UPA is used in place of an $8 \times 8$. Accordingly, ZF and MR respectively experienced on average $\times 2.4$ and $\times 1.9$ multiplexing gain by deploying a higher number of antennas.

## REFERENCES


[1] George Dimitrakopoulos and Panagiotis Demestichas. "Intelligent transportation systems". In: *IEEE Vehicular Technology Magazine* 5.1 (2010), pp. 77–84. DOI: 10.1109/MVT.2009.935537.

[2] Junping Zhang, Fei-Yue Wang, Kunfeng Wang, Wei- Hua Lin, Xin Xu, and Cheng Chen. "Data-driven intelligent transportation systems: A survey". In:IEEE Transactions on Intelligent Transportation Systems 12.4 (2011), pp. 1624–1639. DOI: 10 . 1109/TITS.2011.2158001.

[3] Hamidreza Bagheri, Md Noor-A-Rahim, Zilong Liu, Haeyoung Lee, Dirk Pesch, Klaus Moessner, and Pei Xiao. "5G NR-V2X: Toward connected and cooperative autonomous driving". In: *IEEE Communications Standards Magazine* 5.1 (2021), pp. 48–54. DOI: 10.1109/MCOMSTD.001.2000069.

[4] Mehdi Harounabadi, Dariush Mohammad Soleymani, Shubhangi Bhadauria, Martin Leyh, and Elke Roth-Mandutz. "V2X in 3GPP standardization: NR sidelink in Release-16 and beyond". In: *IEEE Communications Standards Magazine* 5.1 (2021), pp. 12–21. DOI: 10.1109/MCOMSTD.001.2000070.

[5] Zachary MacHardy, Ashiq Khan, Kazuaki Obana, and Shigeru Iwashina. "V2X access technologies: regulation, research, and remaining challenges". In: *IEEE Communications Surveys Tutorials* 20.3 (2018), pp. 1858–1877. DOI: 10 . 1109 / COMST . 2018.2808444.

[6] Pranav Kumar Singh, Sunit Kumar Nandi, and Sukumar Nandi. "A tutorial survey on vehicular communication state of the art, and future research directions". In: *Vehicular Communications* 18 (2019), p. 100164. ISSN: 2214-2096. DOI: 10 . 1016/j.vehcom.2019.100164.

[7] Syed S. Husain, Andreas Kunz, Athul Prasad, Emmanouil Pateromichelakis, and Konstantinos Samdanis. "Ultra-high reliable 5G V2X communications". In: *IEEE Communications Standards Magazine* 3.2 (2019), pp. 46–52. DOI: 10 . 1109 / MCOMSTD.2019.1900008.

[8] Xiaohu Ge. "Ultra-reliable low-latency communications in autonomous vehicular networks". In: *IEEE Transactions on Vehicular Technology* 68.5 (2019), pp. 5005–5016. DOI: 10 . 1109 / TVT . 2019 . 2903793.

[9] Mario H. Castañeda Garcia, Alejandro Molina-Galan, Mate Boban, Javier Gozalvez, Baldomero Coll-Perales, Taylan Şahin, and Apostolos Kousaridas. "A tutorial on 5G NR V2X communications". In: *IEEE Communications Surveys Tutorials* 23.3 (2021), pp. 1972–2026. DOI: 10 . 1109 / COMST . 2021.3057017.

[10] Amitabha Ghosh, Andreas Maeder, Matthew Baker, and Devaki Chandramouli. "5G evolution: A view on 5G cellular technology beyond 3GPP Release 15". In: *IEEE Access* 7 (2019), pp. 127639–127651. DOI: 10.1109/ACCESS.2019.2939938.

[11] Ian F. Akyildiz, Ahan Kak, and Shuai Nie. "6G and beyond: The future of wireless communications systems". In: *IEEE Access* 8 (2020), pp. 133995–134030. DOI: 10.1109/ACCESS.2020.3010896.

[12] Walid Saad, Mehdi Bennis, and Mingzhe Chen. "A vision of 6G wireless systems: Applications, trends, technologies, and open research problems". In: *IEEE Network* 34.3 (2020), pp. 134–142. DOI: 10.1109/MNET.001.1900287.

[13] Mostafa Zaman Chowdhury, Md. Shahjalal, Shakil Ahmed, and Yeong Min Jang. "6G wireless communication systems: applications, requirements, technologies, challenges, and research directions". In: *IEEE Open Journal of the Communications Society* 1 (2020), pp. 957–975. DOI: 10.1109/OJCOMS.2020.3010270.

[14] Thien Thi Thanh Le and Sangman Moh. "Comprehensive survey of radio resource allocation schemes for 5G V2X communications". In: *IEEE Access* 9 (2021), pp. 123117–123133. DOI: 10.1109/ACCESS.2021.3109894.

[15] Yongjun Xu, Guan Gui, Haris Gacanin, and Fumiyuki Adachi. "A survey on resource allocation for 5G heterogeneous networks: current research, future trends, and challenges". In: *IEEE Communications Surveys Tutorials* 23.2 (2021), pp. 668–695. DOI: 10.1109/COMST.2021.3059896.

[16] Shanzhi Chen, Jinling Hu, Yan Shi, Ying Peng, Jiayi Fang, Rui Zhao, and Li Zhao. "Vehicle-to-everything (V2X) services supported by LTE-based systems and 5G". In: *IEEE Communications Standards Magazine* 1.2 (2017), pp. 70–76. DOI: 10.1109/MCOMSTD.2017.1700015.

[17] Mate Boban, Apostolos Kousaridas, Konstantinos Manolakis, Josef Eichinger, and Wen Xu. "Connected roads of the future: use cases, requirements, and design considerations for vehicle-to-everything communications". In: *IEEE Vehicular Technology Magazine* 13.3 (2018), pp. 110–123. DOI: 10.1109/MVT.2017.2777259.

[18] Ahmad Alalewi, Iyad Dayoub, and Soumaya Cherkaoui. "On 5G-V2X use cases and enabling technologies: A comprehensive survey". In: *IEEE Access* 9 (2021), pp. 107710–107737. DOI: 10.1109/ACCESS.2021.3100472.

[19] Marco Giordani, Michele Polese, Marco Mezzavilla, Sundeep Rangan, and Michele Zorzi. "Toward 6G networks: Use cases and technologies". In: *IEEE Communications Magazine* 58.3 (2020), pp. 55–61. DOI: 10.1109/MCOM.001.1900411.

[20] 3GPP TS 22.186 v16.2.0. *3rd Generation Partnership Project; technical specification group services and system aspects; study on enhancement of 3GPP support for 5G V2X services (Release 16)*. 2019.

[21] Azim Eskandarian, Chaoxian Wu, and Chuanyang Sun. "Research advances and challenges of autonomous and connected ground vehicles". In: *IEEE Transactions on Intelligent Transportation Systems 22.2 (2021), pp. 683–711. DOI: 10.1109/TITS.2019.2958352.*

[22] Xiong Wang, Linghe Kong, Fanxin Kong, Fudong Qiu, Mingyu Xia, Shlomi Arnon, and Guihai Chen. "Millimeter wave communication: A comprehensive survey". In: *IEEE Communications Surveys Tutorials* 20.3 (2018), pp. 1616–1653. DOI: 10.1109/COMST.2018.2844322.

[23] Emil Björnson, Luca Sanguinetti, Henk Wymeersch, Jakob Hoydis, and Thomas L. Marzetta. "Massive MIMO is a reality—What is next?: Five promising research directions for antenna arrays". In: *Digital Signal Processing* 94 (2019), pp. 3–20. ISSN: 1051-2004. DOI: 10.1016/j.dsp.2019.06.007.

[24] Junil Choi, Vutha Va, Nuria Gonzalez-Prelcic, Robert Daniels, Chandra R. Bhat, and Robert W. Heath. "Millimeter-wave vehicular communication to support massive automotive sensing". In: *IEEE Communications Magazine* 54.12 (2016), pp. 160–167. DOI: 10.1109/MCOM.2016.1600071CM.

[25] Sherif Adeshina Busari, Kazi Mohammed Saidul Huq, Shahid Mumtaz, Linglong Dai, and Jonathan Rodriguez. "Millimeter-wave massive MIMO communication for future wireless systems: A survey". In: *IEEE Communications Surveys Tutorials* 20.2 (2018), pp. 836–869. DOI: 10.1109/COMST.2017.2787460.

[26] Emil Bjornson, Liesbet Van der Perre, Stefano Buzzi, and Erik G. Larsson. "Massive MIMO in sub-6 GHz and mmWave: Physical, practical, and use-case differences". In: *IEEE Wireless Communications* 26.2 (2019), pp. 100–108. DOI: 10.1109/MWC.2018.1800140.

[27] Filippo Morandi, Francesco Linsalata, Mattia Brambilla, Marouan Mizmizi, Maurizio Magarini, and Umberto Spagnolini. "A probabilistic codebook technique for fast initial access in 6G vehicle-to-vehicle communications". In: *2021 IEEE International Conference on Communications Workshops (ICC Workshops)*. 2021, pp. 1–6. DOI: 10.1109/ICCWorkshops50388.2021.9473772.

[28] Dario Tagliaferri, Mattia Brambilla, Monica Nicoli, and Umberto Spagnolini. "Sensor-aided beamwidth and power control for next generation vehicular communications". In: *IEEE Access* 9 (2021), pp. 56301–56317. DOI: 10.1109/ACCESS.2021.3071726.

[29] Marouan Mizmizi, Francesco Linsalata, and Mattia Brambilla *et al.* "Fastening the initial access in 5G NR sidelink for 6G V2X networks". In: *Vehicular Communications* (2021), p. 100402. ISSN: 2214-2096. DOI: 10.1016/j.vehcom.2021.100402.

[30] Ahmed Alkhateeb, Jianhua Mo, Nuria Gonzalez-Prelcic, and Robert W. Heath. "MIMO precoding and combining solutions for millimeter-wave systems". In: *IEEE Communications Magazine* 52.12 (2014), pp. 122–131. DOI: 10.1109/MCOM.2014.6979963.

[31] Mattia Brambilla, Daniele Pardo, and Monica Nicoli. "Location-assisted subspace-based beam alignment in LOS/NLOS mm-wave V2X communications". In: *2020 IEEE International Conference on Communications (ICC)*. 2020, pp. 1–6. DOI: 10.1109/ICC40277.2020.9148587.

[32] Omar El Ayach, Sridhar Rajagopal, Shadi Abu-Surra, Zhouyue Pi, and Robert W. Heath. "Spatially sparse precoding in millimeter wave MIMO systems". In: *IEEE Transactions on Wireless Communications* 13.3 (2014), pp. 1499–1513. DOI: 10.1109/TWC.2014.011714.130846.

[33] Marco Giordani, Michele Polese, Arnab Roy, Douglas Castor, and Michele Zorzi. "A tutorial on beam management for 3GPP NR at mmWave frequencies". In: *IEEE Communications Surveys Tutorials* 21.1 (2019), pp. 173–196. DOI: 10.1109/COMST.2018.2869411.

[34] Mehdi Haghshenas, Mattia D'Adda, Francesco Linsalata, Luca Barbieri, Monica Nicoli, and Maurizio Magarini. "On the performance of zero-forcing beamforming in a real I2V scenario at millimiter wave". In: *2021 International Balkan Conference on Communications and Networking (BalkanCom)*. 2021, pp. 56–60. DOI: 10.1109/BalkanCom53780.2021.9593210.

[35] *Wireless InSite*. https://www.remcom.com/wireless-insite-em-propagation-software.

[36] Md. Noor-A-Rahim, Zilong Liu, Haeyoung Lee, G. G. Md. Nawaz Ali, Dirk Pesch, and Pei Xiao. "A survey on resource allocation in vehicular networks". In: *IEEE Transactions on Intelligent Transportation Systems* 23.2 (2022), pp. 701–721. DOI: 10.1109/TITS.2020.3019322.

[37] Huaizhou SHI, R. Venkatesha Prasad, Ertan Onur, and I.G.M.M. Niemegeers. "Fairness in wireless networks: issues, measures and challenges". In: *IEEE Communications Surveys Tutorials* 16.1 (2014), pp. 5–24. DOI: 10.1109/SURV.2013.050113.00015.

[38] Hoon Kim and Youngnam Han. "A proportional fair scheduling for multicarrier transmission systems". In: *IEEE Communications Letters* 9.3 (2005), pp. 210–212. DOI: 10.1109/LCOMM.2005.03014.

[39] Mi Yang, Bo Ai, Ruisi He, Zhangfeng Ma, Zhangdui Zhong, Junhong Wang, Li Pei, Yujian Li, Jing Li, and Ning Wang. "Non-stationary vehicular channel characterization in complicated scenarios". In: *IEEE Transactions on Vehicular Technology* 70.9(2021), pp. 8387–8400. DOI: 10.1109/TVT.2021.3096973.

[40] Marwan Yusuf, Emmeric Tanghe, Frédéric Challita, Pierre Laly, Davy P. Gaillot, Martine Liénard, Luc Martens, and Wout Joseph. "Stationarity analysis of V2I radio channel in a suburban environment". In: *IEEE Transactions on Vehicular Technology* 68.12 (2019), pp. 11532–11542. DOI: 10.1109/TVT.2019.2927435.

[41] Fang Li, Wei Chen, and Yishui Shui. "Analysis of non-stationarity for 5.9 GHz channel in multiple vehicle-to-vehicle scenarios". In: *Sensors* 21.11 (2021), p. 3626.

[42] Gongjun Yan and Stephan Olariu. "A probabilistic analysis of link duration in vehicular ad hoc networks". In: *IEEE Transactions on Intelligent Transportation Systems* 12.4 (2011), pp. 1227–1236. DOI: 10.1109/TITS.2011.2156406.

[43] Robert Margolies, Ashwin Sridharan, Vaneet Aggarwal, Rittwik Jana, N. K. Shankaranarayanan, Vinay A. Vaishampayan, and Gil Zussman. "Exploiting mobility in proportional fair cellular scheduling: Measurements and algorithms". In: (2014), pp. 1339–1347. DOI: 10.1109/INFOCOM.2014.6848067.

[44] Taesang Yoo and A. Goldsmith. "On the optimality of multiantenna broadcast scheduling using zero-forcing beamforming". In: *IEEE Journal on Selected Areas in Communications* 24.3 (2006), pp. 528–541. DOI: 10.1109/JSAC.2005.862421.

[45] Qimei Chen, Xiaoxia Xu, and Hao Jiang. "Spatial multiplexing based NR-U and WiFi coexistence in unlicensed spectrum". In: *2019 IEEE 90th Vehicular Technology Conference (VTC2019-Fall)*. 2019, pp. 1–5. DOI: 10.1109/VTCFall.2019.8891514.

[46] Taesang Yoo and A. Goldsmith. "Optimality of zero-forcing beamforming with multiuser diversity". In: *IEEE International Conference on Communications, 2005. ICC 2005. 2005*. Vol. 1. 2005, 542–546 Vol. 1. DOI: 10.1109/ICC.2005.1494410.

[47] Zhenyu Tu and R.S. Blum. "Multiuser diversity for a dirty paper approach". In: *IEEE Communications Letters* 7.8 (2003), pp. 370–372. DOI: 10.1109/LCOMM.2003.815652.

[48] Rui Zhang, J.M. Cioffi, and Ying-Chang Liang. "Throughput comparison of wireless downlink transmission schemes with multiple antennas". In: *IEEE International Conference on Communications, 2005. ICC 2005. 2005*. Vol. 4. 2005, 2700–2704 Vol. 4. DOI: 10.1109/ICC.2005.1494839.

[49] Kyeongjun Ko and Jungwoo Lee. "Low complexity multiuser MIMO scheduling with chordal distance". In: *2008 42nd Annual Conference on Information Sciences and Systems*. 2008, pp. 80–84. DOI: 10.1109/CISS.2008.4558499.

 

[50] Elmahdi Driouch and Wessam Ajib. "A graph theory based scheduling algorithm For MIMO-CDMA systems using zero forcing beamforming". In: *2008 IEEE Symposium on Computers and Communications*. 2008, pp. 674–679. DOI: 10.1109/ISCC.2008.4625665.

[51] Liutong Du, Lihua Li, Hien Quoc Ngo, Trang C. Mai, and Michail Matthaiou. "Cell-free massive MIMO: Joint maximum-ratio and zero-forcing precoder with power control". In: *IEEE Transactions on Communications* 69.6 (2021), pp. 3741–3756. DOI: 10.1109/TCOMM.2021.3059300.

[52] Constantine A Balanis. *Antenna theory: analysis and design*. Wiley-Interscience, 2005.

[53] Emil Björnson, Jakob Hoydis, and Luca Sanguinetti. "Massive MIMO Networks: Spectral, Energy, and Hardware Efficiency". In: *Foundations and Trends in Signal Processing* 11.3-4 (2017), pp. 154–655. ISSN: 1932-8346. DOI: 10.1561/2000000093.

[54] David Tse and Pramod Viswanath. *Fundamentals of wireless communication*. Cambridge university press, 2005.

[55] Aldebaro Klautau, Pedro Batista, Nuria González-Prelcic, Yuyang Wang, and Robert W. Heath. "5G MIMO data for machine learning: Application to beam-selection using deep learning". In: *2018 ITA Workshop*. 2018, pp. 1–9. DOI: 10.1109/ITA.2018.8503086.

[56] Pablo Alvarez Lopez et al. "Microscopic Traffic Simulation using SUMO". In: *2018 21st International Conference on Intelligent Transportation Systems (ITSC)*. IEEE, 2018.

[57] OpenStreetMap contributors. *Planet dump retrieved from https://planet.osm.org*. https://www.openstreetmap.org. 2017.

## AUTHORS

**Mehdi Haghshenas** received a B.Sc. (2015) in electrical enginnering from the Islamic Azad University of Tehran, and an M.Sc. (2020) in telecommunication engineering from the Politecnico di Milano. Currently, he is pursuing his Ph.D. degree in information technology at the Politecnico di Milano. His research interests include mmWave communication, massive MIMO, and reconfigurable intelligent surfaces.

**Francesco Linsalata** received B.Sc. and M.Sc. degrees cum laude in telecommunication engineering from the Politecnico di Milano, Milan, Italy, in 2017 and 2019, respectively. Currently, he is a Ph.D .student at the Dipartimento di Elettronica, Informazione e Bioingegneria, Politecnico di Milano. His main research interests focus on V2X communications and waveform design for B5G wireless networks. He was the co-recipient of the best paper award and recipient of the best student paper award at BalkanCom'19.

**Luca Barbieri** received B.Sc. and M.Sc. (cum laude) degrees in telecommunication engineering from the Politecnico di Milano in 2017 and 2019, respectively. He is currently a Ph.D. student in information technology at Dipartimento di Elettronica, Informazione e Bioingegneria (DEIB), Politecnico di Milano. His current research interests focus on machine learning and localization techniques for vehicular and industrial networks.

**Mattia Brambilla** received B.Sc (2015) and M.Sc (2017) degrees in telecommunication engineering and a Ph.D. degree (2021) in information technology from the Politecnico di Milano. He was a visiting researcher with the NATO Centre for Maritime Research and Experimentation (CMRE), La Spezia, Italy, in 2019. In 2021, he joined the Faculty of Dipartimento di Elettronica, Informazione e Bioingegneria (DEIB), Politecnico di Milano, as a research fellow. He was the recipient of the Best Student Paper Award at the 2018 IEEE Statistical Signal Processing Workshop. His research interests include signal processing, statistical learning, and data fusion for cooperative localization and vehicular communication.

**Monica Nicoli** received M.Sc. (Hons.) and Ph.D. degrees in communication engineering from the Politecnico di Milano, 1802 Milan, Italy, in 1998 and 2002, respectively. She was a visiting researcher with ENI Agip, from 1998 to 1999, and Uppsala University, Uppsala, Sweden, in 2001. In 2002, she joined the Politecnico di Milano as a faculty member. She is currently an associate professor in telecommunications with the Department of Management, Economics and Industrial Engineering. Her research interests include signal processing, machine learning, and wireless communications, with emphasis on smart mobility and Internet of Things (IoT) applications. She was the recipient of the Marisa Bellisario Award, in 1999, and a co-recipient of the best paper awards of the IEEE Symposium on Joint Communications and Sensing, in 2021, the IEEE Statistical Signal Processing Workshop, in 2018, and the IET Intelligent Transport Systems Journal, in 2014. She is an associate editor for IEEE Transactions on Intelligent Transportation Systems. She was an associate editor for the EURASIP Journal on Wireless Communications and Networking, from 2010 to 2017, and a lead guest editor for the Special Issue on Localization in Mobile Wireless and Sensor Networks, in 2011.

**Maurizio Magarini** received M.Sc. and Ph.D. degrees in electronic engineering from the Politecnico di Milano, Milan, Italy, in 1994 and 1999, respectively. In 1994, he was granted the TELECOM Italia scholarship award for his M.Sc. thesis. He worked as a research associate in the Dipartimento di Elettronica, Informazione e Bioingegneria at the Politecnico di Milano from 1999 to 2001. From 2001 to 2018, he was an assistant professor in Politecnico di Milano where, since June 2018, he has been an associate professor. From August 2008 to January 2009 he spent a sabbatical at Bell Labs, Alcatel-Lucent, Holmdel, NJ. His research interests are in the broad area of communication and information theory. Topics include synchronization, channel estimation, equalization and coding applied to wireless and optical communication systems. His most recent research activities have focused on molecular communications, massive MIMO, study of waveforms for 5G cellular systems, vehicular communications, wireless sensor networks for mission critical applications, and wireless networks using unmanned aerial vehicles and high-altitude platforms. He has authored and coauthored more than 100 journal and conference papers. He was the co-recipient of two best paper awards. He is an associate editor of IEEE Access, IET Electronics Letters, and Nano Communication Networks (Elsevier). He has been involved in several European and national research projects.